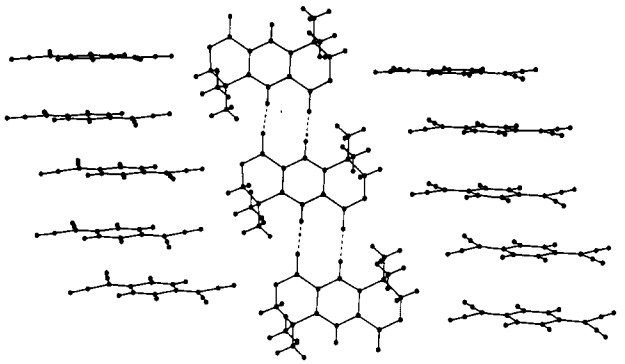

Figure 2. Packing diagram of the TCNQ salt of 1. The short intermolecular O-H distances are shown as dotted lines.

Table I. Bond Lengths and Angles for the Central Ring of 1 and 2

	bond lengths, Å			bond angles, deg	
	1	2		1	2
N(5)-C(6)	1.443 (1)	1.393 (3)	N(5)-C(6)-C(7)	119.5 (1)	119.3 (2)
C(6)-C(7)	1.343 (2)	1.355 (3)	C(6)-C(7)-N(5a)	123.9 (1)	122.4 (2)
N(5)-C(7a)	1.351 (2)	1.343 (3)	C(6)-N(5)-C(7a)	116.3 (1)	118.3 (2)

Cyclic voltammetry on a solution of 1 in methylene chloride with tetrabutylammonium perchlorate supporting electrolyte revealed two reversible oxidation waves at -0.33 V and 0.61 V vs ferrocene/ferricinium corresponding to oxidation of 1 to the radical cation 2 and dication 3, respectively. The former was characterized by its five-line ESR signal (relative intensity 1:2:3:2:1, $g = 2.0035$, $a_N = 6.9$ G) when an acetonitrile solution of 1 was oxidized with 1 equiv of ferrin, $[Fe(phen)_3]^{3+}$. The high stability of 2 (calculation gives $K_{disproportionation} = 1.5 \times 10^{-16}$) is probably due in part to captodative stabilization[11] or merostabilization[12] and also to the high coulombic destabilization of 3 and the "antiaromatic destabilization" of 1.

When 1 was added to 1 equiv of TCNQ in hot acetonitrile under an inert atmosphere, an emerald green, paramagnetic, air-sensitive solution was formed, presumably containing 2 and the TCNQ radical anion. An ESR spectrum of this solution revealed only a broad unresolved signal. Upon slow cooling of the solution, purplish-black, opaque needles were deposited having the stoichiometry $DDTTA(TCNQ)_2$. X-ray analysis of a single crystal (Figure 2) revealed chains of stacked TCNQ dimers with "ribbons" of 2 aligned edge to edge in between the chains. Within these ribbons, the distance between the carbonyl oxygen and ring hydrogen on a neighboring molecule is rather short (2.38 Å), suggesting a small "edge on" interaction along the ribbon. At ambient temperature the TCNQ chains exhibit a Peierls distortion, which gives rise to the semiconducting nature of the material.[1] Initial (two-probe) measurements gave a room temperature conductivity on the order of 10^{-3} Ω^{-1} cm^{-1}. Measurement of the degree of charge transfer[13] gave $Z = 0.57$ per TCNQ molecule. Interestingly, this corresponds to a positive charge of 1.14 per DDTTA molecule. The central ring of the DDTTA became planar and the N(5)-C(6) bond became shorter by 0.05 Å as DDTTA became "partially aromatic" (Table I). The mean deviation of the six central ring atoms from a least-squares plane is now 0.001 Å.

Though the electrical properties of this complex are not exceptional, the donor represents an interesting new organic structure with three stable one-electron redox states. Electron acceptors other than TCNQ may give rise to higher conductivities. Variation of the substitution on the 1,4-dihydro-2,5-bis(alkoxycarbonyl)-pyrazine unit may lead to further novel CT complexes and provide insight into the electronic structure of this interesting chromophore.

Acknowledgment. We gratefully acknowledge financial support from the NSF in the form of Grant CHE-8903637, Dr. H. M. Duan and Dr. Allen Hermann for conductivity measurements, and Dr. Cortlandt Pierpont for use of his cyclic voltammetry apparatus.

Supplementary Material Available: A complete description of the X-ray crystallographic determinations of 1 and the TCNQ salt of 1 including atomic coordinates, isotropic and anisotropic displacement parameters, bond lengths, bond angles, and torsion angles (17 pages); listing of observed and calculated structure factors for 1 and the TCNQ salt of 1 (10 pages). Ordering information is given on any current masthead page.

(11) Stella, L.; Janousek, Z.; Merényi, R.; Viehe, H. G. *Angew. Chem., Int. Ed. Engl.* **1978**, *17*, 691. Viehe, H. G.; Janousek, Z.; Merényi, R.; Stella, L. *Acc. Chem. Res.* **1985**, *18*, 148.
(12) Baldock, R. W.; Hudson, P.; Katritzky, A. R. *J. Chem. Soc., Perkin Trans. 1* **1974**, 1422. Katritzky, A. R.; Zerner, M. C.; Karelson, M. M. *J. Am. Chem. Soc.* **1986**, *108*, 7213.
(13) Chappell, J. S.; Bloch, A. N.; Bryden, W. A.; Maxfield, M.; Poehler, T. O.; Cowan, D. O. *J. Am. Chem. Soc.* **1981**, *103*, 2442.

Pulsed Endor Study of the Native and High pH Perturbed Forms of the Blue Copper Site in Stellacyanin

Hans Thomann,*,† Marcelino Bernardo,† Michael J. Baldwin,‡ Michael D. Lowery,‡ and Edward I. Solomon*,‡

Corporate Research Laboratory
EXXON Research and Engineering Company
Annandale, New Jersey 08801
Department of Chemistry, Stanford University
Stanford, California 94305
Received August 9, 1990

The spectroscopic properties and electronic structure of type 1 (T1) copper sites in blue copper proteins have been intensively studied.[1-3] In the prototypical blue copper proteins plastocyanin[4] and azurin,[5] where X-ray crystal structures have been published, the chromophore is $Cu[N(HIS)]_2S(CYS)S(MET)$ in a distorted T_d coordination geometry. Stellacyanin, a blue Cu protein isolated from the Japanese lacquer tree, *Rhus vernicifera*, is unusual in several respects.[6] Stellacyanin has no protein methionine residues, has the lowest redox potential (+184 mV) of all blue copper proteins, and exists in a reversible perturbed form between pH 9 and 11.5 which has slightly different spectral properties but still has T1 character.[6,7] Neither the fourth ligand on copper which replaces the thioether sulfur ligand in the normal blue copper sites nor the nature of the high pH perturbed form is known.

In this communication, we present data from pulsed ENDOR and a new two-dimensional pulsed electron nuclear electron triple resonance method for recording hyperfine selective ENDOR (HS-ENDOR) spectra[8,9] on the native (pH 6.4) and high pH (pH 11.0) perturbed forms of the blue Cu site in stellacyanin. ENDOR lines for two imino imidazole nitrogens and two strongly coupled methylene protons from a cysteine thiolate ligand are observed at both pH 6.4[10] and pH 11.0. A third nitrogen coupling is observed at pH 11. This fourth ligand, which exhibits much larger hyperfine anisotropy than imidazole imino nitrogen couplings,[10,11]

†EXXON Research and Engineering Company.
‡Stanford University.

(1) Malkin, R.; Malmstrom, B. G. *Adv. Enzymol.* **1970**, *33*, 177-244.
(2) Fee, J. A. *Struct. Bonding (Berlin)* **1975**, *23*, 1-60.
(3) Gray, H. B.; Solomon, E. I. In *Copper Proteins*; Spiro, T. G., Ed.; Wiley-Interscience: New York, 1981.
(4) Colman, P. J.; Freeman, H. C.; Guss, J. M.; Murata, M.; Norris, V. A.; Ramshaw, J. A. M.; Venkatappa, M. P. *Nature (London)* **1978**, *272*, 319-324.
(5) Norris, G. E.; Anderson, B. F.; Baker, E. N. *J. Am. Chem. Soc.* 1986, *108*, 2784-2785.
(6) Peisach, J.; Levine, W. G.; Blumberg, W. E. *J. Biol. Chem.* **1967**, *242*, 2847-2858.
(7) Malmstrom, B. G.; Reinhammer, B.; Vanngard, T. *Biochim. Biophys. Acta* **1970**, *205*, 48-57.
(8) Thomann, H.; Bernardo, M. *Chem. Phys. Lett.* **1990**, *169*, 5-11.
(9) Buhlmann, C.; Schweiger, A.; Ernst, R. R. *Chem. Phys. Lett.* **1989**, *154*, 285-291.
(10) Roberts, J. E.; Cline, J. F.; Lum, V.; Freeman, H. C.; Gray, H. B.; Peisach, J.; Reinhammer, B.; Hofmann, B. M. *J. Am. Chem. Soc.* **1984**, *106*, 5324-5330.

0002-7863/91/1513-5911$02.50/0

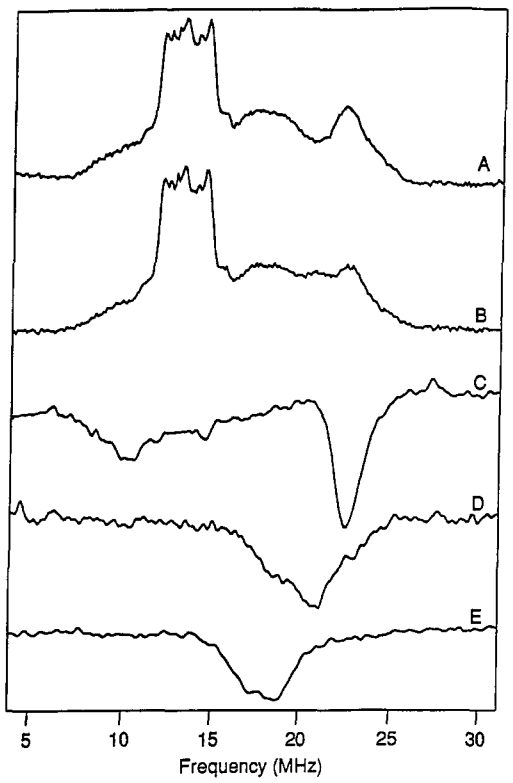

Figure 1. ENDOR and HS-ENDOR spectra for the native (A) and high pH (B–E) forms of stellacyanin. Experimental conditions: observation frequency, 9.0800 GHz; magnetic field, 3134.1 G; T = 1.65 K; rf pulse width, 8.00 μs; microwave π pulse width, 0.10 μs; microwave inversion pulse frequency, (C) 9.0610 GHz, (D) 9.0382 GHz, (E) 9.0440 GHz. Other conditions: sample concentration, 1 mM; sample volume, 0.07 mL; resolution, 0.1 MHz/point; sweep rate, 40 ms/point; 30 echoes sampled/point; total sweeps, (A) 22, (B) 12, (C) 132, (D) 60, (E) 218.

is assigned as an amide nitrogen. Thus at high pH the active site in stellacyanin is Cu[N(HIS)]$_2$S(CYS)N(amide).

Pulsed ENDOR spectra were recorded by using a pulse sequence proposed by Davies.[12,13] These are the pulsed analogues of spectra recorded by the conventional method of continuous-wave excitation.[14] However, spectra recorded by the pulsed method are less susceptible to line-shape and line-position distortions arising from spin relaxation and rapid passage effects.[15] This permits a more precise measurement of the hyperfine coupling parameters.

Pulsed ENDOR spectra of stellacyanin at pH 6.4 and 11.0 are shown in parts A and B, respectively, of Figure 1. The more intense peaks centered at 12.5 MHz (the proton Larmor frequency) arise from protons on coordinated imidazole ligands[11] and from protons on nearby protein residues.[10] The broader peaks centered at 9.5 and 17.5 MHz have been assigned to the imino nitrogen couplings from two coordinated imidazole ligands.[10,16] The peak at 22 MHz has been assigned to a strongly coupled proton resonance[10,16] from the methylene group of a cysteine thiolate ligand.[17] It has been suggested that it also involves a resonance from a nitrogen with an anisotropic hyperfine coupling.[18] In addition, a broader line is observed at 21 MHz in Figure 1B, which is not evident in Figure 1A. We have used a new two-dimensional pulsed ENDOR method to determine whether this resonance and the resonance at 22 MHz arise from protons or nitrogen.[19]

HS-ENDOR spectra were recorded by using a pulsed electron nuclear electron triple resonance technique.[8,9] It is analogous to the method of Davies ENDOR except that two microwave frequencies, separated by Δ, are used for the excitation and detection microwave pulses. A hyperfine selective ENDOR spectrum is recorded for a given nucleus with hyperfine coupling A when $\Delta = A$. Thus Δ preselects the nucleus to be observed; other nuclei do not contribute to that HS-ENDOR spectrum. Each HS-ENDOR spectrum is therefore a slice out of a two-dimensional ENDOR spectrum where the rf frequency defines one axis and Δ defines the other axis.

Several HS-ENDOR spectra of stellacyanin at pH 11.0 are shown in Figure 1C–E. Two resonances are observed in the HS-ENDOR spectrum recorded when Δ = 19 MHz, which arise from nuclei with A = 19 MHz. The line at 22 MHz must arise from a proton coupling since it is at a frequency $A/2$ above the proton Larmor frequency.[20,21] Note that a second proton resonance at 23.5 MHz in Figure 1A,B, which corresponds to A = 22 MHz, does not contribute to Figure 1C. The 22- and 23.5-MHz proton resonances are assigned to the methylene protons of a coordinated cysteinyl protein residue.[10,16,17] The amplitudes of these resonances vary by 50% depending on the g value at which the ENDOR spectra are recorded.[24] This indicates hyperfine anisotropy and accounts for the low intensity of the resonance at 23.5 MHz in Figure 1B. The other resonance in Figure 1C at 9.5 MHz must arise from a nitrogen nucleus with A = 19 MHz since it is centered at $A/2$. Similarly, the peak at 17.5 MHz observed when Δ = 36 MHz (Figure 1E) must arise from a nitrogen nucleus with A = 35 MHz. The splitting by twice the nitrogen Larmor frequency is evident (1.2 MHz) while no nitrogen quadrupole splitting is detected, consistent with previous reports.[10,16,17] These two nitrogen couplings are assigned to the imidazole imino nitrogens from protein histidinyl residues.

The new resonance at 21 MHz present only in the high pH form of stellacyanin (Figure 1B) is observed in the HS-ENDOR spectrum when Δ = 42 MHz (Figure 1D), indicating that it does arise from a nitrogen (A = 42 MHz). Since the two imidazole imino nitrogens and cysteinyl methylene protons are observed with identical frequencies and amplitudes at pH 6.4 and 11.0, the resonance at 21 MHz must arise from a third nitrogen, i.e., a fourth ligand. The intensity of the ENDOR line from this third nitrogen varies by 50% for ENDOR spectra collected between g_z and g_x.[24] This indicates considerable hyperfine anisotropy and suggests that this third nitrogen resonance does not arise from an imino nitrogen of an imidazole ligand. The latter are known

(11) Van Camp, H. L.; Sands, R. H.; Fee, J. A. *J. Chem. Phys.* **1981**, *75*, 2098–2107.
(12) Davies, E. R. *Phys. Lett.* **1974**, *47A*, 1–4.
(13) The Davies pulse sequence consists of a three-pulse inversion recovery microwave pulse sequence in which a radio-frequency pulse is applied between the first and second microwave pulses. The pulsed ENDOR spectrum is recorded by plotting the echo intensity as function of rf frequency and incrementing the frequency on successive pulse sequence iterations. The ENDOR signal is detected as a change in the amplitude of an electron spin echo formed by the second and third microwave pulses.
(14) Feher, G. *Phys. Rev.* **1956**, *103*, 843.
(15) Weger, M. *Bell Syst. Tech. J.* **1960**, *39*, 1013.
(16) Rist, G. H.; Hyde, J. S.; Vanngard, T. *Proc. Natl. Acad. Sci. U.S.A.* **1970**, *67*, 79–86.
(17) Stevens, T. H.; Martin, C. T.; Wang, H.; Brudvig, G. W.; Scholes, C. P.; Chan, S. I. *J. Biol. Chem.* **1982**, *257*, 12106–12113.
(18) Roberts, J. E.; Brown, T. G.; Hoffman, B. M.; Peisach, J. *J. Am. Chem. Soc.* **1980**, *102*, 825–829.
(19) The analysis of ENDOR spectra of blue copper proteins recorded at X-band microwave frequencies is usually complicated by the overlap of strongly coupled nitrogen and weakly coupled proton ENDOR lines.[10,16] The overlap of the proton and nitrogen resonances can be eliminated by recording the ENDOR spectra at higher microwave excitation frequencies.[20,22] The proton resonance lines shift with the proton Larmor frequency while strongly coupled nitrogen lines remain centered at one-half the hyperfine coupling frequency. However, the overlap of ENDOR resonances arising from nitrogens with similar hyperfine couplings will not be eliminated by recording spectra at higher microwave excitation frequencies. This can be achieved by using the hyperfine selective ENDOR method.
(20) The proton ENDOR frequencies are given by $\nu_\pm^H = |\nu_H \pm A^H/2|$ where ν_H is the free proton Larmor frequency and A^H is the hyperfine coupling. This relation is valid for $A^H/2 < \nu_H$ and gives a pair of lines symmetrically displaced about ν_H. The nitrogen ENDOR frequencies are given by $\nu_N = |A^N/2 \pm \nu_N + (2m-1)(3P^N/2)|$ where P is the quadrupole coupling and $-I+1 \le m \le I$. This relation is valid for $A/2 > \nu_N > 3P^N/2$.
(21) The low-frequency partner expected at 3.0 MHz is difficult to detect because of the weak hyperfine enhancement factor at low rf frequency.[23]
(22) Werst, M. M.; Davoust, C. E.; Hoffman, B. M. *J. Am. Chem. Soc.* **1991**, *113*, 1533–1538.
(23) Bleaney, B.; Abragam, A. *Electron Paramagnetic Resonance of Transition Metal Ions*; Clarendon: Oxford, 1970.
(24) Thomann, H.; Bernardo, M.; Solomon, E. I., unpublished results.

to have only a 10% hyperfine anisotropy in Cu complexes.[10,11] Hyperfine couplings of similar magnitude and anisotropy have been observed for nitrogen couplings in Cu(II)-amide complexes.[25]

A resonance Raman line at 1234 cm^{-1}, characteristic of a simultaneous C-N stretch and N-H bend, is observed in the high pH form of stellacyanin.[26] The intensity of this line grows with increasing pH, and it is in resonance with the 600-nm absorption band, indicating that it arises from the blue Cu site. On the basis of these combined results, we conclude that a nitrogen of an amide ligand is a fourth ligand coordinated to Cu in the high pH perturbed blue form of stellacyanin. One interesting explanation for the appearance of a deprotonated amide coordinated to the blue copper site involves a linkage isomerization of the amide, from carbonyl oxygen to amide nitrogen at high pH as is observed in Cu-amide model chemistry.[27] The amide ligand provides a stronger ligand field than the thioether sulfur bond present in other blue Cu sites, which is consistent with the unique spectroscopic (i.e., rhombic split EPR[28]) and redox properties (i.e., low potential) that distinguish stellacyanin from other blue Cu proteins. This $Cu[N(HIS)]_2S(CYS)N(amide)$ model for the active site in stellacyanin is also consistent with recent molecular modeling predictions.[29] Detailed spectroscopic studies on the low and high pH forms of stellacyanin are presently underway.

Acknowledgment. The portion of this work performed at Stanford University was supported by NSF Grant CHE8919687.

(25) Calvo, R.; Oseroff, S. B.; Abache, H. C. *J. Chem. Phys.* **1980**, *72*, 760-767.
(26) Penfield, K. W. Ph.D. Thesis, Massachusetts Institute of Technology, Cambridge, MA, 1984.
(27) Margerum, D. W.; Wong, L. F.; Bossu, F. P.; Chellappa, K. L.; Czarnecki, J. J.; Kirksey, S. T., Jr.; Neubecker, T. A. *Adv. Chem. Ser.* **1977**, *162*, 281-303.
(28) Gewirth, A.; Cohen, S.; Schugar, H.; Solomon, E. I. *Inorg. Chem.* **1987**, *26*, 1133.
(29) Fields, B. A.; Guss, J. M.; Freeman, H. C., unpublished results.

Selective Formation of Molecular Oxygen/Perfluoro Crown Ether Adduct Ions in the Gas Phase

Jennifer Brodbelt,* Simin Maleknia, Chien-Chung Liou, and Richard Lagow

Department of Chemistry, University of Texas at Austin Austin, Texas 78712-1167
Received October 1, 1990

The abilities of crown ethers to form complexes with alkali cations and organic molecules has generated long-term interest[1-4] in host-guest chemistry.[5] Likewise this interest has extended to the coordination abilities of perfluorinated macrocyclic analogues which exhibit decreased basicities and have different pocket size dimensions. Some biocompatible perfluorinated compounds have high oxygen-carrying capacity[6] and have demonstrated great potential as artificial blood components.[7] From a physiological standpoint, the mechanism of oxygen binding to the fluoro ethers is particularly intriguing but poorly understood. We report herein preliminary results on the selective formation and structural characterization of oxygen/perfluoro crown ether negatively charged complexes in the gas phase.

The perfluoro crown ethers, synthesized via the LaMar direct fluorination procedure,[8,9] were admitted into the source of a triple-quadrupole mass spectrometer via a variable leak valve. The hydro crown ethers were introduced via a direct probe. Argon was introduced into the source manifold at 2-3 × 10^{-6} Torr to aid in the production of thermal electrons for electron-capture negative ionization. The desired reagent gas (CO, CO_2, air for O_2) was added to attain a total manifold pressure of 3.0-9.0 × 10^{-6} Torr, or a source pressure of 1-2 Torr using a chemical-ionization ion volume. The ethers examined included perfluoro-12-crown-4, perfluoro-15-crown-5, perfluoro-18-crown-6, the hydro crown analogues, and an acyclic ether, $CF_3(CF_2)_3(OCF_2CF_2)_2OCF_2(OCF_2CF_2)_2O(CF_2)_3CF_3$.

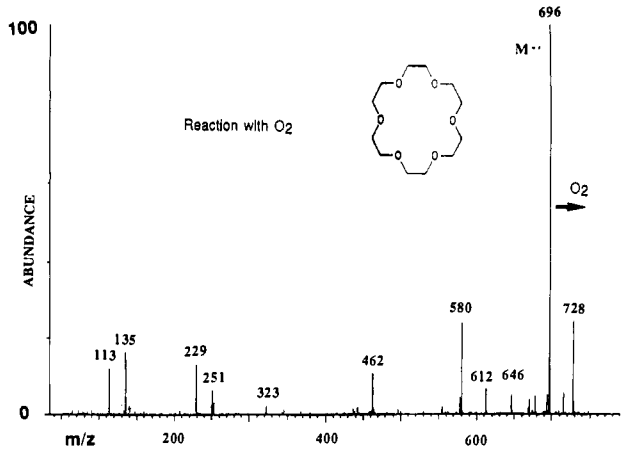

Figure 1. Negative-ionization mass spectrum of perfluoro-18-crown-6 and oxygen.

Figure 1 shows the negative-ionization mass spectrum for the reaction products of perfluoro-18-crown-6 (molecular weight 696) with oxygen. An abundant adduct ion is observed at m/z 728 due to $(M + 32)^{\bullet-}$. This ion is not observed in the absence of oxygen in the source. The $(M + O_2)^{\bullet-}$ adduct ion is observed for the other perfluorinated crown ethers with an abundance of 20-60% relative to the molecular ion. The capability for oxygen adduct formation was also evaluated for the nonfluorinated crown ethers. Adducts with O_2 were *never* observed, either in the positive or negative ionization modes.

Additionally, the abilities of the perfluoro crown ethers to form complexes with CO, CO_2, and Ar, species with sizes and some properties similar to those of O_2, were examined. Adducts with these species were not observed in either the positive or negative ionization modes. Thus, the tendencies of the perfluoro crown ethers to form adducts exhibit striking selectivity for O_2 only. The nonfluorinated ethers do not form adducts with any of these molecules either.

Ion/molecule reactions involving *acyclic* perfluoro ethers were also examined to determine whether the cyclic nature of the crown ethers played a role in the formation of the $(M + O_2)^{\bullet-}$ adducts. The acyclic ether, $CF_3(CF_2)_3(OCF_2CF_2)_2OCF_2(OCF_2CF_2)_2O(CF_2)_3CF_3$, did not form $(M + O_2)^{\bullet-}$ adducts. This suggests that the macrocyclic nature of the perfluoro crown ethers enhances binding to O_2.

In order to elucidate whether the perfluoro crown ether negative *ions* were reacting with neutral O_2 or crown ether *neutrals* were reacting with $O_2^{\bullet-}$, the two substrates were introduced into separate regions of the triple-quadrupole instrument so that selective ion/molecule reactions could be performed. For these experiments, 5 mTorr of O_2 was admitted into the second quadrupole region, which also may serve as a reactive collision chamber. The perfluoro crown ether was ionized in the source, and then the mass-selected molecular ion, $M^{\bullet-}$, was passed through the reaction quadrupole at a kinetic energy of 6 eV. Abundant $(M + O_2)^{\bullet-}$ adducts were observed in the resulting mass spectrum, indicating that crown ether negative *ions* may attach to *neutral* O_2.

Structural details of the perfluoro ether ions, $M^{\bullet-}$, and their O_2 adduct ions, $(M + O_2)^{\bullet-}$, were probed via collisionally activated dissociation (CAD) of the mass-selected parent ions. Argon was used as the target gas at 1.0 mTorr. Figure 2 shows the 30-eV CAD spectra of the molecular ion ($M^{\bullet-}$) of the perfluoro-18-

(1) Dang, L.; Kollman, P. *J. Am. Chem. Soc.* **1990**, *112*, 5716.
(2) Dietrich, B.; Lehn, J.-M.; Sauvage, J. *Tetrahedron Lett.* **1969**, 2885.
(3) De Boer, J.; Reinhoudt, D.; Harkema, S.; van Hummel, G.; de Jong, F. *J. Am. Chem. Soc.* **1982**, *104*, 4073.
(4) De Jong, F.; Reinhoudt, D. *Adv. Phys. Org. Chem.* **1980**, *17*, 279.
(5) Cram, D. *Science* **1988**, *240*, 760.
(6) Reiss, J.; LeBlanc, M. *Angew. Chem., Int. Ed. Engl.* **1978**, *17*, 621.
(7) Weiss, R. *Sci. News* **1987**, *132*, 200.
(8) Huang, H.; Lagow, R. *Bull. Soc. Chim. Fr.* **1986**, 993.
(9) Lin, W.; Bailey, W.; Lagow, R. *J. Chem. Soc., Chem. Commun.* **1985**, 1350.

0002-7863/91/1513-5913$02.50/0